Altered orbitofrontal tissue microstructure in patients with chronic anterior temporal lobe lesions

Soyoung Choi[1], Chitresh Bhushan[1], Anand A. Joshi[1], Kristin Raphel[1], Daniel Tranel[2], David W. Shattuck[3], Justin P. Haldar[1], Richard M. Leahy[1], Hanna Damasio[1], Jessica L. Wisnowski[1,4]

[1]University of Southern California, Los Angeles, CA, United States
[2]University of Iowa, Iowa City, IA, United States
[3]University of California Los Angeles, Los Angeles, United States
[4]University of Pittsburgh, Pittsburgh, PA, United States

Introduction:

The anterior temporal lobe (ATL) is strongly interconnected with the frontal lobe, particularly the orbitofrontal cortex (OFC) and, to a lesser extent, the cingulate and lateral frontal cortex, via direct fiber pathways in the uncinate faciculus and extreme capsule (Schmahmann & Pandya, 2006). Given this pattern of connectivity, an important unanswered question is: what secondary effect does an ATL lesion have on the microstructure-and ultimately, the underlying connectivity-of the frontal lobe? We hypothesized tissue microstructure would be altered of the OFC ipsilateral to chronic ATL lesions as evidenced by diffusion tensor imaging (DTI).

Subjects:

12 adult subjects (all right-handed) with ATL lesions (n= 7, right; 5, left) due to surgical resection (n=9) or hemorrhage (n=3) underwent MRI (T1-weighted, DTI) scans as part of large-scale project on focal brain lesions (NIH NS019632). The imaging data was retrieved from the Iowa-USC Patient Registry.

Extraction and Segmentation in Lesion Data:

3D-T1-weighted MRI scans (MPRAGE; 1mm isotropic voxels) were processed using BrainSuite (Shattuck & Leahy, 2002) to produce cortical surface meshes and tissue classification maps; this processing was performed in a semi-automated fashion, with limited manual correction of the cortical boundaries to minimize extraneous inclusion of meninges or cerebellum into the cerebral volumes. Lesion brain images were then segmented into 90 regions of interest (ROIs) by applying an automated algorithm, SVReg, to the extracted brain meshes and corresponding MRI data (Joshi, Shattuck, & Leahy, 2012). SVReg uses two criteria (surface curvature and the 3D location of vertices in the cortical surface mesh) to align a single subject atlas which has been segmented into anatomical ROIs by an expert, to a target brain (here, the lesion subject). Although local curvature information is destroyed in the vicinity of a cortical lesion, the preservation of the curvature in the remaining tissue and the availability of cortical surface vertex locations adjacent to the damaged tissue stabilizes the alignment to the reference brain and therefore allows for segmentation of lesioned brains.

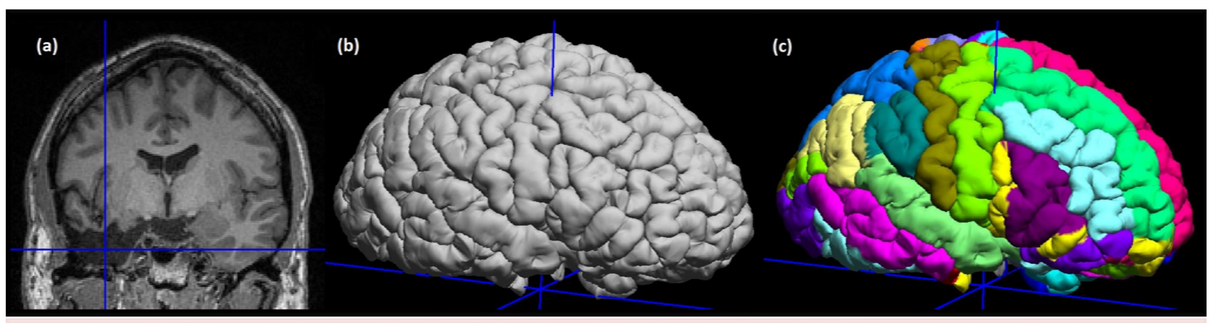

Figure 1: (a) Coronal cross-sectional view of the lesion in the right ATL. (b) Surface rendering of same subject after processing in BrainSuite. (c) Labeled ROIs displayed on surface above after coregistration of template brain with SVReg (Note: Cross-hairs indicate the location of the lesion)

Diffusion Processing:

For each subject, DTI data (TE=86 ms; TR=11000 ms; FOV: 256x256 mm^2; 2 mm isotropic voxels; 64 diffusion-encoding directions at b-value = 1000 s/mm^2) were corrected for geometric distortion using the acquired fieldmap before diffusion tensor estimation and then aligned to T1-weighted images using BrainSuite Diffusion Pipeline (Bhushan, Haldar, Joshi & Leahy, 2012). The anatomical ROIs, further segmented into gray matter (GM) and white matter (WM), were then mapped to the DTI data. (Fig. 2)

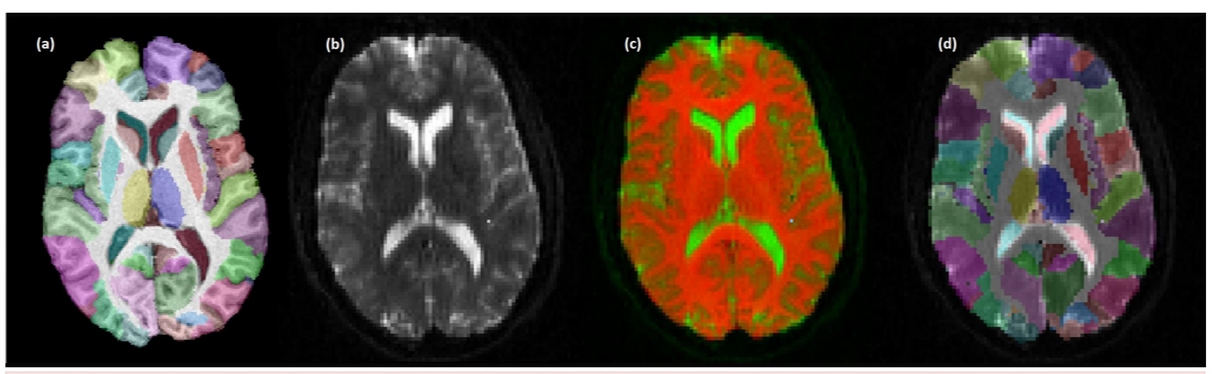

Figure 2:
(a) Labeled ROIs displayed on skull-stripped T1-weighted image for one subject. (b) Fieldmap corrected b=0 s/mm^2 image from diffusion data for the same subject. (c) Overlay of corrected b=0 s/mm^2 image (in green) and skull-stripped T1-weighted image (in red). (d) Labeled ROIs displayed on corrected b=0 s/mm^2 image.

Data Analysis:

DTI metrics (FA, MD, axial [AD] and radial diffusivity [RD]) were computed voxelwise and mean values were computed for each ROI, separately for GM and WM. Paired t-tests (SPSS; IBM corporation) were used to compare DTI metrics obtained ipsilateral versus contralateral to the ATL lesion within 7 frontal ROIs selected a priori for this study (Fig. 3). Significance was thresholded at $p < 0.05$, uncorrected.

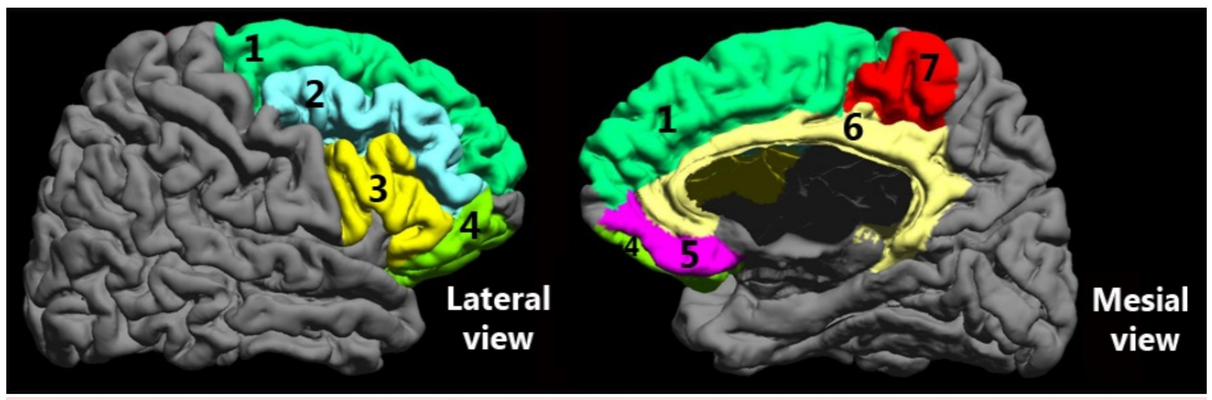

Figure 3: Displayed above on lateral and mesial views of the right hemisphere of the atlas template are the 7 ROIs included in this study: 1. Superior frontal gyrus (SFG) 2. Middle frontal gyrus (MFG) 3. Inferior frontal gyrus (IFG) 4. Orbitofrontal cortex (OFC) 5. Gyrus rectus (GR) 6. Cingulate (Cing) 7. Paracentral lobule (ParaCL)

Results:

MD, AD and RD values were significantly higher in the GM and the WM (MD and RD only) of the OFC ipsilateral to the ATL lesion relative to the homologous contraleral ROI. FA was lower in the same regions (Table 1.) Diffusivity was also increased in the GM of the IFG and in the WM of the MFG, and FA was decreased in the WM of the IFG (Table 1).

	Gray Matter				White Matter			
	MD	AD	RD	FA	MD	AD	RD	FA
SFG								
MFG					↑*		↑*	
IFG	↑*	↑*	↑*					↓**
Cing								
ParaCL								
GR								
OFC	↑**	↑**	↑**	↓**	↑*		↑**	↓*

Table 1: Significant results. Arrows indicate the directionality of the results with up arrows indicating significantly higher values in the ipsilateral ROI relative to the homologous contralateral ROI and down arrows indicating smaller values.
* $p < 0.05$ ** $p<0.01$

Conclusions:

In a cohort of patients with circumscribed lesions involving the ATL, we observed microstructural differences in distal GM and WM regions of the ipsilateral frontal lobe relative to homologous regions in the contralateral hemisphere. Consistent with the known connectivity, these differences were most prominent in the OFC in comparison to other frontal regions. These results suggest that the microstructure of the OFC has been altered as a result of an ATL lesion. Further research is needed to understand whether these secondary structural changes affect the function of the orbitofrontal cortex in patients with anterior temporal lesions.

All processing for this study, described in methods section, was performed using BrainSuite. For more information or to download the software, please visit the BrainSuite website: http://brainsuite.loni.ucla.edu/
Tutorials and sample data are also available on our website

References

[1]Schmahmann, J.D., Pandya, D.N. (2006), "Fiber Pathways of the Brain," Oxford University Press. pp. 419-425.
[2]Shattuck, D.W. and Leahy, R.M. (2002) "BrainSuite: An Automated Cortical Surface Identification Tool," Medical Image Analysis, 8(2):129-142.
[3]Joshi, A.A., Shattuck, D.W., Leahy, R.M. (2012) "A Fast and Accurate Method for Automated Cortical Surface Registration And Labeling," WBIR'12 Proceedings of the 5th International Conference on Biomedical Image Registation, pp. 180-189.
[4] Bhushan C., Haldar, J.P., Joshi, A.A., Leahy, R.M. (2012) "Correcting Susceptibility-Induced Distortion in Diffusion-Weighted MRI using Constrained Nonrigid Registration," 2012 APSIPA Annual Summit and Conference, pp.1-9